American Journal of Engineering and Applied Sciences

Original Research Paper

Singularity Analysis of a Hybrid Serial-Cable Driven Planar Robot

[1]Samir Lahouar and [2]Lotfi Romdhane

[1]LGM, Ecole Nationale d'Ingénieurs de Monastir, Université de Monastir, Monastir, Tunisia
[2]Department of Mechanical Engineering, College of Engineering, American University of Sharjah, Sharjah, United Arab Emirates

Article history
Received: 13-07-2022
Revised: 13-08-2022
Accepted:19-08-2022

Corresponding Author:
Samir Lahouar
LGM, Ecole Nationale d'Ingénieurs de Monastir, Université de Monastir, Monastir, Tunisia
Email: samirlahouar@gmail.com

Abstract: In this study, we address the problem of singularities of a hybrid serial-cable driven planar robot. Based on an analytical kinetostatic analysis three types of singularities are determined, i.e., serial, parallel, and combined singularities. In addition, cable tensions should be positive, otherwise, the robot will be uncontrollable. The serial singularity corresponds to positions where the serial port of the robot is fully extended or fully folded. The parallel singularity corresponds to aligned cables and combined singularities correspond to both cases. Cable tensions distribution, within the workspace, is determined, which allowed the identification of regions where the cable tensions exceed an allowable value. The influence of physical parameters on the workspace of the robot and its singular configurations is also studied. An example of a gait rehabilitation system using this type of robot is shown. Based on the kinetostatic analysis, multi-objective optimization of the dexterity and the cable tensions is performed, which yielded solutions represented by a Pareto front. The results have been extended to the case of 3 degrees of freedom hybrid robot.

Keywords: Hybrid Serial-Cable Driven Planar Robot Singularities Lower Limb Rehabilitation

Introduction

Cable-driven robots with passive support are a special case of robots combining the advantages of parallel robots and those of serial robots (Trevisani *et al*., 2006; Pigani and Gallina, 2014). The serial part provides stiffness normal to the plane of motion, which means that the robot is suspended by cables rather than being supported. The passive joints in the serial part can be equipped with sensors, which improves the precision of the robot, especially when high masses and accelerations are involved. These robots are lightweight and have a high payload and a large workspace.

Singularities are well studied in the case of serial and parallel robots (Litvin and Parenti, 1985; Gosselin and Angeles, 1990; Yang *et al*., 2002; Bonev *et al*., 2003; Firmani and Podhorodeski, 2009; Liu *et al*., 2012). Most of these works study the Jacobian matrices of the robot. A singularity is detected when there is a loss of rank in those matrices. For serial robots, singularities correspond to the limits of the workspace where some of the geometrical inverse solutions meet (Litvin and Parenti, 1985). However, for closed-loop mechanisms, there are three main groups of singularities (Gosselin and Angeles, 1990) Serial singularities correspond to the case where the chain reaches a limit of the workspace or an internal limit of a branch of the closed chain. The second kind of singularity is a parallel singularity, which usually corresponds to the case where the gripper is locally movable even if the actuators are locked. These singularities can occur within the workspace. The third kind is the combined singularity (Gosselin and Angeles, 1990) where the two previous singularities occur simultaneously.

To deal with singularities and to avoid dangerous positions for the robot, several works are focused on determining a singularity-free workspace within a prescribed region. This is done by varying geometrical parameters (Zou *et al*., 2012; Li *et al*., 2016). Other works detect singular configurations during the path planning process. In (Lahouar *et al*., 2008) singularities of parallel robots were treated as obstacles and were avoided during path planning generation. This method was extended to cable-driven robots (Lahouar *et al*., 2009; Ismail *et al*., 2016). Several other authors validate prescribed trajectories by optimizing the time

or the force (Boudreau and Nokleby, 2012; Barnett and Gosselin, 2015; Trevisani, 2013; Zhang and Shang 2016). Although singular configurations can be crossed during the motion of the robot, these positions cannot be initial or final. Detecting static singular configurations is helpful to avoid using these configurations as start and final positions. Cable tensions are evaluated dynamically during the motion without knowing the shape of the singularity-free workspace and without knowing the distribution of the cable tensions in the workspace. In this study, the singularity-free workspace is studied and the cable tensions are evaluated. The dexterity in the workspace is also studied as a function of certain geometric parameters of the robot. To evaluate dexterity, some studies used the determinant of the Jacobian matrix (Paul and Stevenson, 1983). In (Angeles and López-Cajún, 1992) the conditioning index is used. It is defined as the reciprocal of the condition number of the homogeneous Jacobian matrix. Yoshikawa proposed the manipulability index (Yoshikawa, 1985). Many other studies use the condition number of the Jacobian matrix as a dexterity measure (Zargarbashi *et al*., 2012).

Although singularity and cable tension-related problems are well studied in the literature, to the best of our knowledge, this is the first paper where they are investigated simultaneously. This subject is worthy of investigation to understand the workspace of this kind of robot and its possible use in lower limb rehabilitation.

Kinetostatic Analysis

The studied robot is shown in Fig. 1. It corresponds to a hybrid serial-cable driven planar robot. The serial part is composed of two passive revolute joints. Two cables are attached on one side to the tip of the serial port and attached on the other side to two pulleys actuated by two motors. Figure 1 shows the geometrical parameters of the studied robot as well as the applied forces. P1 and P2 correspond to the weights of links 1 and 2 of the serial part of the robot. Cables are considered nonextensible and their weight is neglected. T_1 and T_2 correspond to tensions in the cables applied at the tip of the serial part. Using a kinetostatic analysis can give an idea about both singularities and cable tensions, which is, in our opinion, better than using the usual velocity relationships.

Applying equilibrium equations on bodies 1 and 2 gives the following equations:

$$\sum_{i=0,2,P_1}\{T_{i\to 1}\}=\{0\},\sum_{i=1,P_2,T_1,T_2}\{T_{i\to 2}\}=\{0\} \quad (1)$$

The reaction forces and moments in the revolute joints correspond to wrenches, which can be written as:

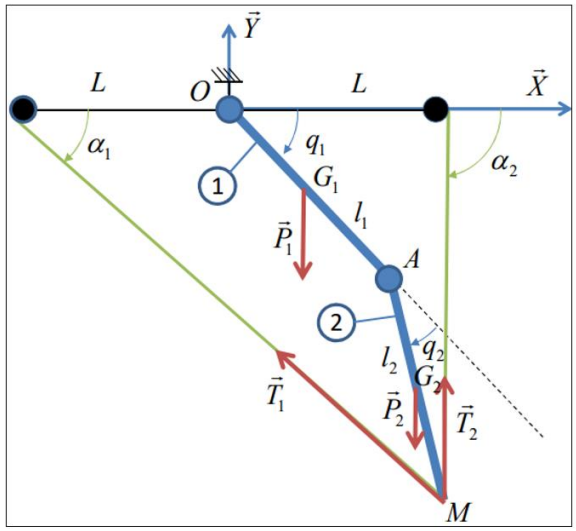

Fig.1: Geometrical parameters and applied forces for the Hybrid serial-cable robot:

$$\{T_{0\to 1}\}=\begin{Bmatrix}X_{01} & 0\\ Y_{01} & 0\\ 0 & 0\end{Bmatrix}_O \quad \{T_{2\to 1}\}=\begin{Bmatrix}X_{21} & 0\\ Y_{21} & 0\\ 0 & 0\end{Bmatrix}_A \quad (2)$$

The weights of link 1 and link 2 are applied in the middle of each bar:

$$\{P_1\}=\begin{Bmatrix}0 & 0\\ -m_1 g & 0\\ 0 & 0\end{Bmatrix}_{G_1} \quad \{P_2\}=\begin{Bmatrix}0 & 0\\ -m_2 g & 0\\ 0 & 0\end{Bmatrix}_{G_2} \quad (3)$$

where, g is the gravity constant and m_1 is the mass of bar 1. Putting the previous screws at the same point O gives the following equation system:

$$\begin{cases} X_{01}+{}_{21}=0 \\ Y_{01}+Y_{21}=m_1 g \\ -1_1\sin q_1 X_{21}+1_1\cos q_1 Y_{21}=\dfrac{1_1}{2}m_1 g\cos q_1 \end{cases} \quad (4)$$

The tension of each cable applies a force at the tipping point M given by the following screw:

$$\{T_i\}=\begin{Bmatrix}-T_i\cos\alpha_i & 0\\ -T_i\sin\alpha_i & 0\\ 0 & 0\end{Bmatrix}_M \quad (5)$$

Equations of equilibrium of body 2 can be written as follow:

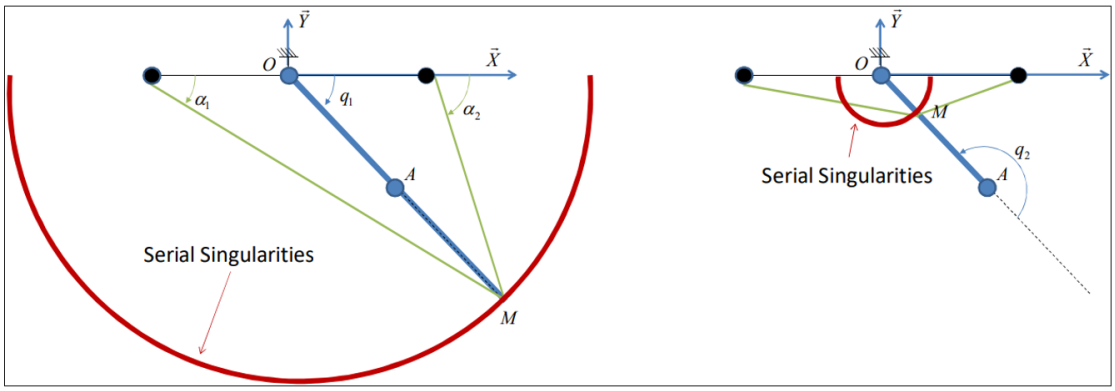

Fig. 2: Serial singularities

$$\begin{cases} -X_{21} - T_1\cos\alpha_1 - T_2\cos\alpha_2 = 0 \\ -Y_{21} - T_1\sin\alpha_1 - T_2\sin\alpha_2 = m_2 g \\ 1_2\sin(q_1+q_2-\alpha_1)T_1 + 1_2\sin(q_1+q_2-\alpha_2)T_2 = \frac{1_2}{2}m_2 g\cos(q_1+q_2) \end{cases} \quad (6)$$

Putting together Eq. (4) and Eq. (6) in a matrix form we obtain:

$$[A]\begin{pmatrix} X_{01} \\ Y_{01} \\ X_{21} \\ Y_{21} \\ T_1 \\ T_2 \end{pmatrix} = \begin{pmatrix} 0 \\ m_1 g \\ \frac{1_1}{2}m_1 g\cos q_1 \\ 0 \\ m_2 g \\ \frac{1_2}{2}m_2 g\cos(q_1+q_2) \end{pmatrix} \quad (7)$$

where:

$$[A] = \begin{bmatrix} 1 & 0 & 1 & 0 & 0 & 0 \\ 0 & 1 & 0 & 1 & 0 & 0 \\ 0 & 0 & -1_1\sin q_1 & 1_1\cos q_1 & 0 & 0 \\ 0 & 0 & -1 & 0 & -\cos\alpha_1 & -\cos\alpha_2 \\ 0 & 0 & 0 & -1 & -\sin\alpha_1 & -\sin\alpha_2 \\ 0 & 0 & 0 & 0 & 1_2\sin(q_1+q_2+\alpha_1) & 1_2\sin(q_1+q_2+\alpha_2) \end{bmatrix} \quad (8)$$

Solving Eq. (7) yields the unknown forces applied to the robot and especially the cable tensions needed to detect singularities. Cable tension values have to be positive to ensure the stability of the robot.

Singularities and Negative Cable Tensions

Singularities occur when det[A] = 0. The det[A] can be written as follows:

$$\det[A] = 1_1 1_2 \sin q_2(\alpha_2 - \alpha_1) \quad (9)$$

Three cases can be considered where det[A] = 0. These singularities are serial, parallel, and combined.

Serial Singularities

The first case of singularity occurs when sin q = 0, which means that $q_2 = 0$ or $q_2 = \pi$ as shown in Fig. 2, the serial port is in full extension or completely replied.

This type of singularity defines the limits of the workspace of the robot. Indeed, as the robot is fully extended, point M generates a circle defining the outer limits of the workspace. However, since the actuation is through the cables, not all the circle is feasible.

Parallel Singularities

These singularities occur when sin $(\alpha_2 - \alpha_1) = 0$, which yields $\alpha = \alpha + k\pi$ as shown in Fig. 3.

Combined Singularities

These singularities occur when there are both types of singularities, serial and parallel. In this case, we have l = l as shown in Fig 4.

Negative Cable Tensions

Cable tensions have to stay non-negative at all times. Solving Eq. (7) gives the values of the tensions:

$$T_1 = \frac{g}{2\sin q_2 \sin(\alpha_2 - \alpha_1)\left[(m_1+m_2)\cos q_1 \sin(q_1+q_2+\alpha_2) + m_2\cos\alpha_2\sin q_2\right]} \quad (10)$$

$$T_2 = \frac{-g}{2\sin q_2 \sin(\alpha_2 - \alpha_1)\left[(m_1+m_2)\cos q_1 \sin(q_1+q_2-\alpha_1) + m_2\cos\alpha_1\sin q_2\right]} \quad (11)$$

When these tensions become negative ($T_1 \le 0$ *or* $T_2 \le 0$), the motors are no longer capable of driving the robot. In this case, the robot fails to execute the required task. It is also worth mentioning here that the two cases, where the tensions in the cables become infinite, are $q_2 = 0$ or $\alpha = \alpha + k\pi$. These cases correspond to the previous three cases, where the robot is in either parallel, serial, or combined singular configuration.

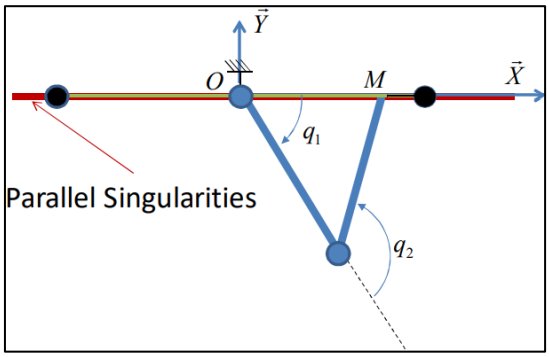

Fig. 3: Parallel singularities

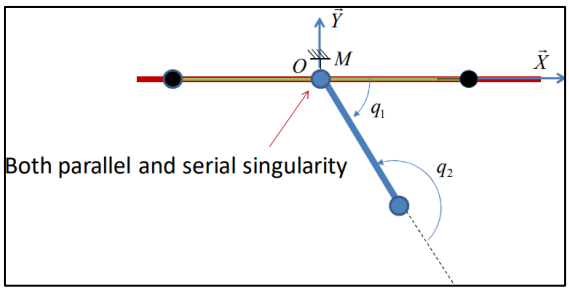

Fig. 4: Combined singularities

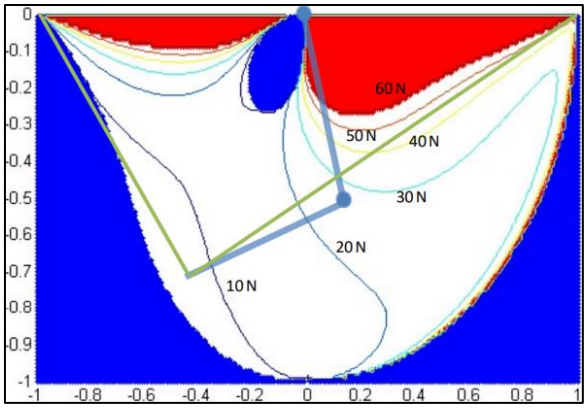

Fig. 5: Free workspace elbow up

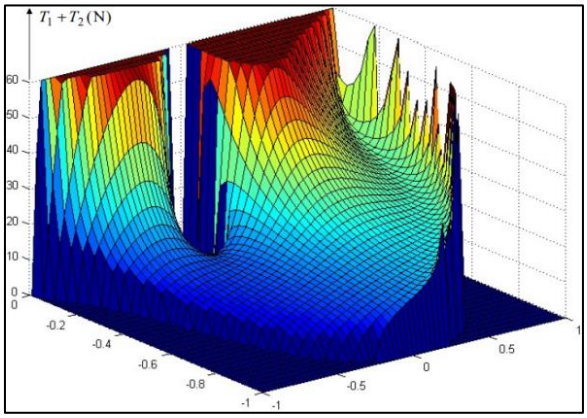

Fig. 6: Tensions in the workspace for elbow up

Simulation Results

To illustrate this analysis, the following parameters were used: g = 9.8 N/kg, L = 1 m, $l_1 = l_2$ = 0.5 and $m_1 = m_2$ = 1 kg. The position of the tip of the robot was modified to span a rectangle as follows: $-1 < x < 1$ and $0 < y < 1$. Figure 5 shows the results of the feasible workspace (in white) of an elbow-up configuration of the robot. Indeed, the serial passive part of the robot has two possible configurations for a given position of the tip, i.e., elbow up and elbow down. It is worth mentioning that the second possible solution (elbow down) yields the mirror image of the vertical axis of the workspace shown in Fig. 4. In what follows, only the elbow-up solution is shown. It is worth mentioning that the robot cannot cross the x-axis without going through a singular configuration. Therefore, it is recommended to define the feasible workspace only on one side of the x-axis. For the application of rehabilitation, the robot will always be below the x-axis. The blue zone corresponds to a non-accessible region due to the drop of the tensions in the cables below a certain limit. Since the value of the sum of the two tensions is monitored, one has to make sure that both tension values stay above a certain minimum value, and the non-accessible region is defined by $T_{min} < T_i < T_{max}$, i = 1, 2. The red zone corresponds to configurations where the cable tensions are greater than a maximum value (i.e., $T_i > T_{max}$, i = 1, 2 and $T_{max} = 60\ N$). This maximum tension ensures that the cable is not broken under excessive tension. Isovalues of tensions (T_1+T_2) is given in Newton to show the distribution of the cable tensions in the workspace.

A 3D representation of the sum of tensions (T_1+T_2) is given in Fig. 6.

The distribution of the tension T_1 in the workspace is shown in Fig. 7, whereas the one for tension T_2 is shown in Fig. 8.

By observing Eq. (10) and (11) it is clear that the shape of the tension distribution within the workspace depends on $\lambda = \frac{m_1}{m_2}$ (the mass ratio). Figure 9 shows the evolution of the workspace depending on λ while keeping $m_1 + m_2$ = 2 kg. It is observed that the singular region decreases when λ increases. This observation means that if m_1 is greater than m_2, then the singular positions due to negative tensions in the cables are reduced.

Gait Assisting Robot

The objective of this section is to present a case study where a robot assists a patient in his gait. The mechanism has to be designed for three objectives.

The first one is related to the workspace to be attained by the tip, which corresponds to the workspace required to move the leg of a patient standing in the upright position. This study space is defined by a rectangle a × b as shown in Fig. 10.

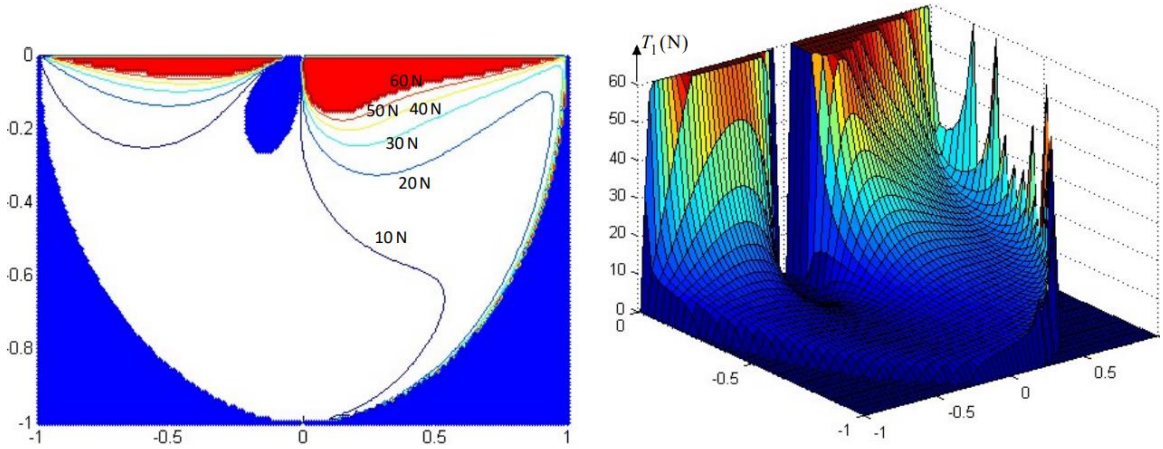

Fig. 7: Tensions T1 in the workspace for elbow up

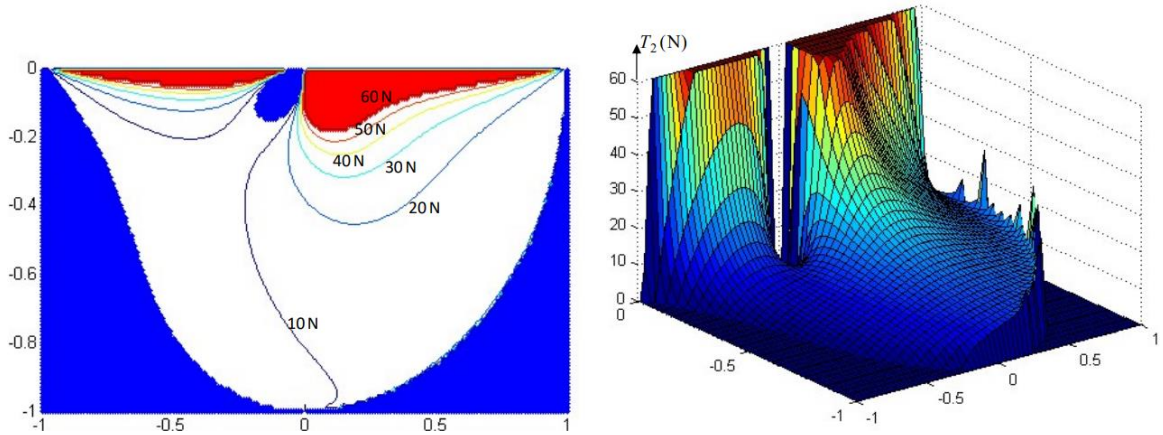

Fig. 8: Tensions T2 in the workspace for elbow up

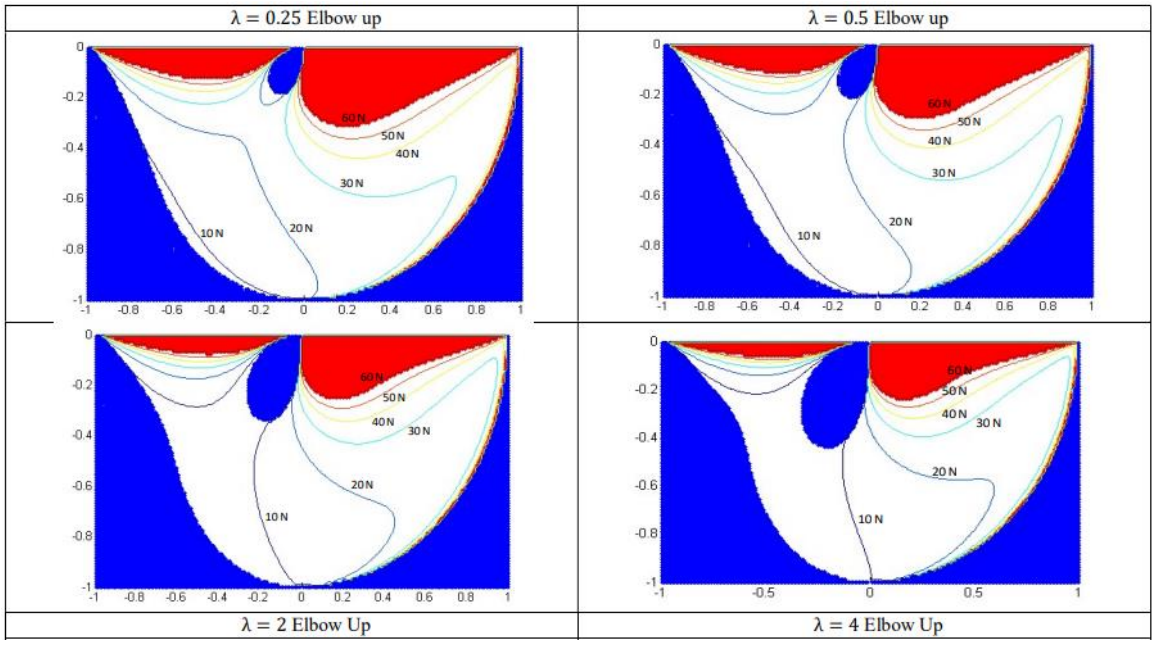

Fig. 9: Workspace and tensions depending on λ

DOI: 10.3844/ajeassp.2022.197.208

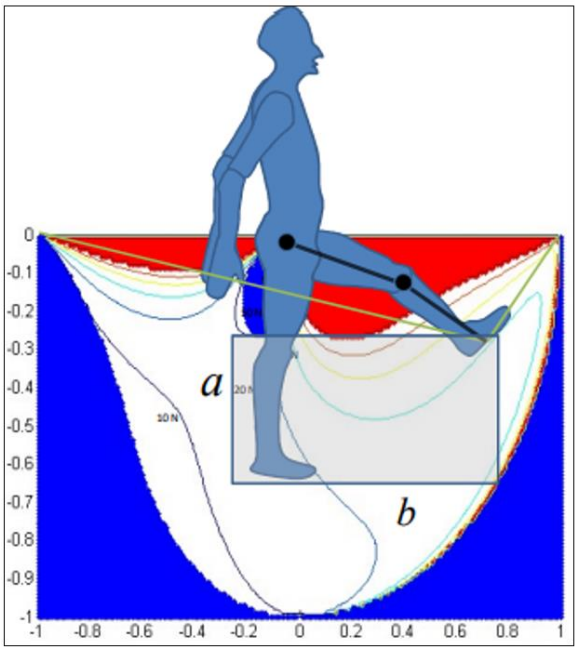

Fig. 10: Gait Assisting robot

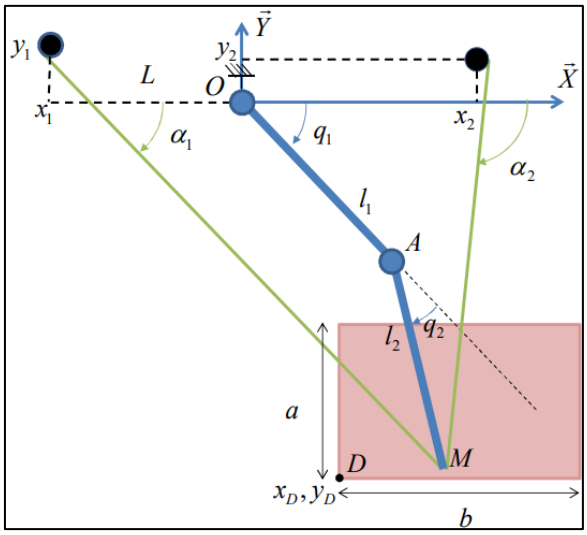

Fig. 11: Parameters optimization for gait rehabilitation

The second objective is to maximize the dexterity of the mechanism within the desired workspace. The dexterity is given by the inverse of the condition number of the matrix [A]. Figure 12 shows the evolution of the condition number depending on L (Fig. 1), and the position of the cable pulleys (Fig. 11). Where λ = 1 and all other parameters are the same as in the last section.

The third constraint is to minimize the required tension values in the cables within the desired workspace. Since the serial passive robot is going to be used to move the full leg, its geometry is to be determined as a function of the person's height.

The parameters to be optimized are the positions of the motors and the height. Figure 11 shows the parameters to be optimized, i.e., the positions of the motors optimized *x*, *y*, *x*, *y* and the height given by *x*, *y*, for a given lengths l, l and the accessible region defined by a, b.

The optimization process has been tested for the following values.

$l_1 = l_2 = 0.5\ m$, $x = -0.3\ m$, $y = -0.7\ m$, a = 0.3 *m* and $b = 0.9\ m$.

Figure 13 shows the Pareto front resulting from minimizing the dexterity and minimizing the average cable tensions in the prescribed region. The optimization method is based on an elitist-controlled genetic algorithm provided by Matlab (Deb, 2011). The population size is 300, the number of generations is 1200, the crossover fraction is 0.8 and the Pareto fraction is 0.5 and the initial penalty is 0.01. This Pareto front shows that minimizing the cable tensions minimizes also the inverse of the condition number of the Jacobian matrix. Table 1 gives three solutions from the Pareto front. These solutions are shown in Fig. 14, 15, and 16.

The best individual in terms of dexterity (solution 1 from the Pareto front) is represented in Fig. 14. It is interesting to note that the obtained solution is not symmetric concerning the y-axis. This result is mainly because the serial robot is in the elbow-up configuration.

In Fig. 15, the results for minimizing cable tensions are shown (solution 2 from the Pareto Front).

We note that this result is close to singular positions as the goal here is to minimize cable tensions and in singular positions, some cable tensions are near 0.

Figure 16 shows results in solution 3. This solution as shown in the Pareto front is the best compromise as it reduces significantly the cable tensions without a noticeable change in dexterity.

Case of the 3 Degrees of Freedom Hybrid Robot

In this section, we apply the same method for the 3 degrees of freedom hybrid robot shown in Fig. 17.

In this example, a link is added to support the foot of the patient. This link is actuated using a third cable. The kineostatic study of this robot gives the following equations:

$$\left[A_2\right]\begin{pmatrix} X_{01} \\ Y_{01} \\ X_{21} \\ Y_{21} \\ T_1 \\ T_2 \\ X_{32} \\ X_{32} \\ T_3 \end{pmatrix} = \begin{pmatrix} 0 \\ m_1 g \\ \frac{1_1}{2} m_1 g \cos q_1 \\ 0 \\ m_2 g \\ \frac{1_2}{2} m_2 g \cos(q_1 + q_2) \\ 0 \\ m_3 g \\ \frac{1_3}{2} m_3 g \cos(q_1 + q_2 + q_3) \end{pmatrix} \quad (12)$$

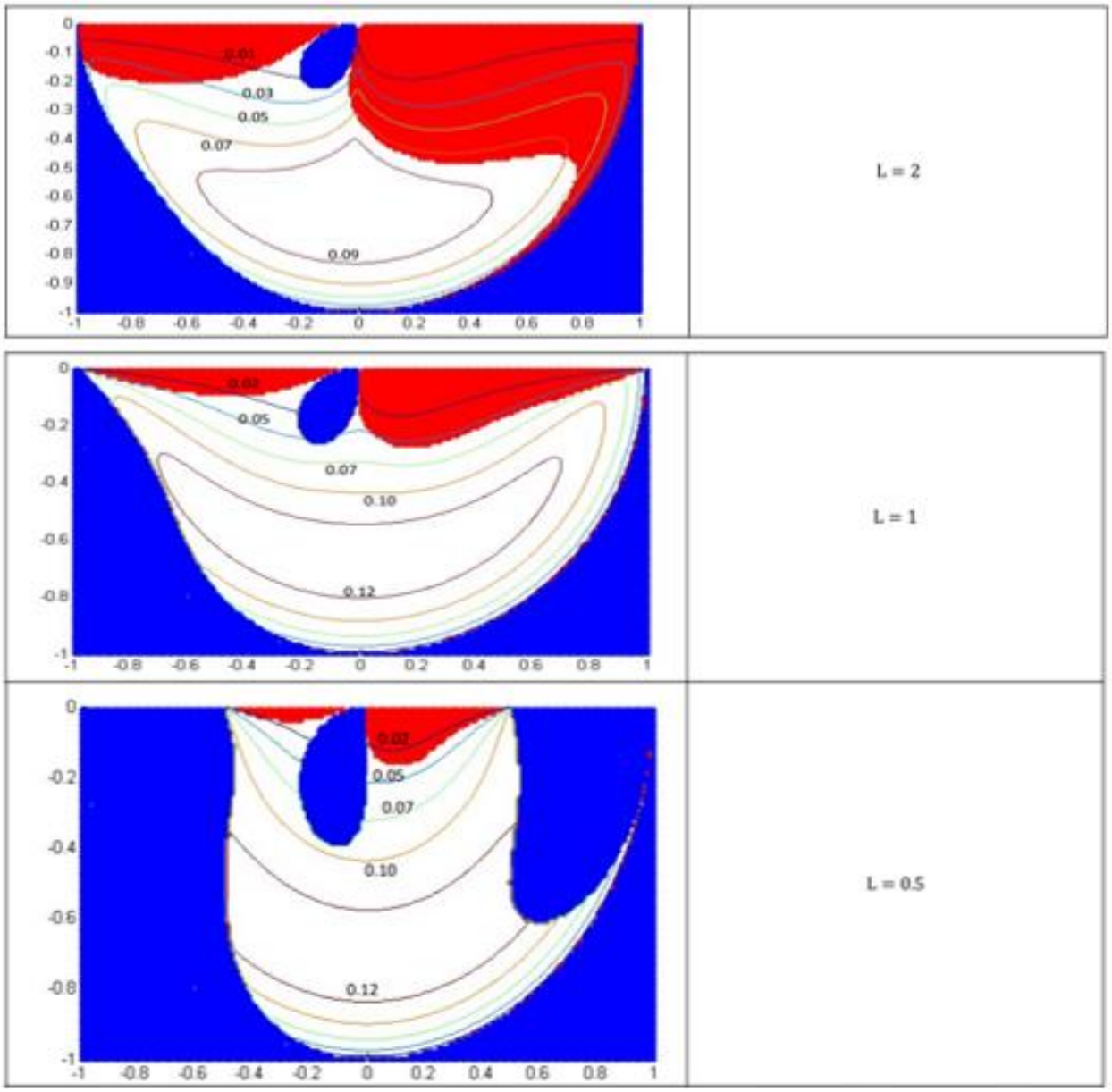

Fig. 12: Evolution of condition number as a function of L

where:

$$\left[A_2\right]=\begin{bmatrix} 1 & 0 & 1 & 0 & 0 & 0 & 0 & 0 & 0 \\ 0 & 1 & 0 & 1 & 0 & 0 & 0 & 0 & 0 \\ 0 & 0 & -1_1\sin q_1 & 1_1\cos q_1 & 0 & 0 & 0 & 0 & 0 \\ 0 & 0 & -1 & 0 & -\cos\alpha_1 & -\cos\alpha_2 & 1 & 0 & 0 \\ 0 & 0 & 0 & -1 & -\sin\alpha_1 & -\sin\alpha_2 & 0 & 1 & 0 \\ 0 & 0 & 0 & 0 & 1_2\sin(q_1+q_2-\alpha_1) & 1_2\sin(q_1+q_2-\alpha_2) & 1_2\sin(q_1+q_2) & 1_2\cos(q_1+q_2) & 0 \\ 0 & 0 & 0 & 0 & 0 & 0 & -1 & 0 & -\cos\alpha_3 \\ 0 & 0 & 0 & 0 & 0 & 0 & 0 & -1 & -\sin\alpha_3 \\ 0 & 0 & 0 & 0 & 0 & 0 & 0 & 0 & 1_3\sin(q_1+q_2-q_3-\alpha_3) \end{bmatrix} \quad (13)$$

Computing the determinant of this matrix gives the following result:

$$\det\left[A_2\right] = l_1 l_2 l_3 \sin q_2 \sin(\alpha_2 - \alpha_1)\sin(q_1 + q_2 + \alpha_3) \quad (14)$$

In this simulation we kept the same values as the previous robot, we just added the values of l_3= 0.2 m and m_3= 0.5 kg.

The Pareto front of the 3 dof hybrid robot is shown in Fig18. Values of average tensions in the cables are not significant as the chosen masses of the links are in the range of 1 Kg max. Average dexterity changes up to 20% between solutions 1 and 2. These solutions are given in Table 2.

Figure 19 shows solution 1 which corresponds to the maximum dexterity in the workspace.

Maximizing the dexterity gives results as far as possible from singularities. This was the same case for the 2 dof hybrid robot.

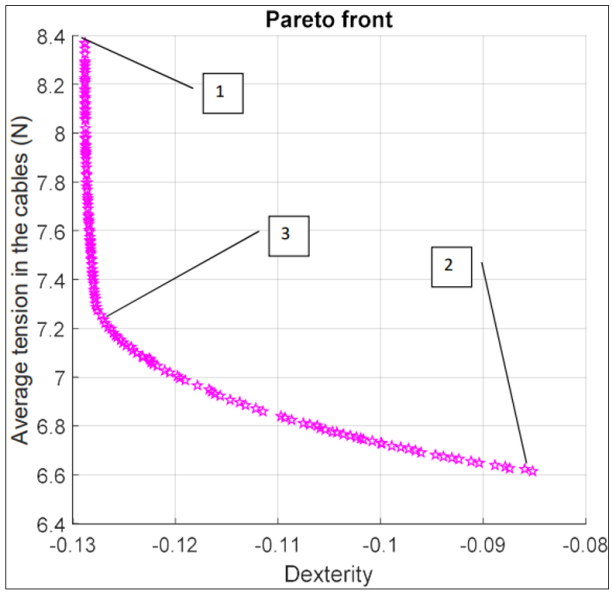

Fig. 13: Pareto front

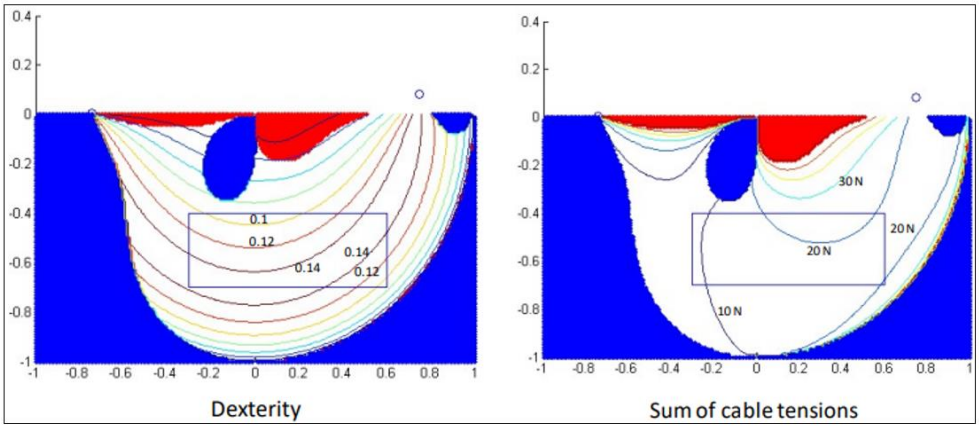

Fig. 14: Results of the optimization process maximizing the inverse of the condition number (solution 1)

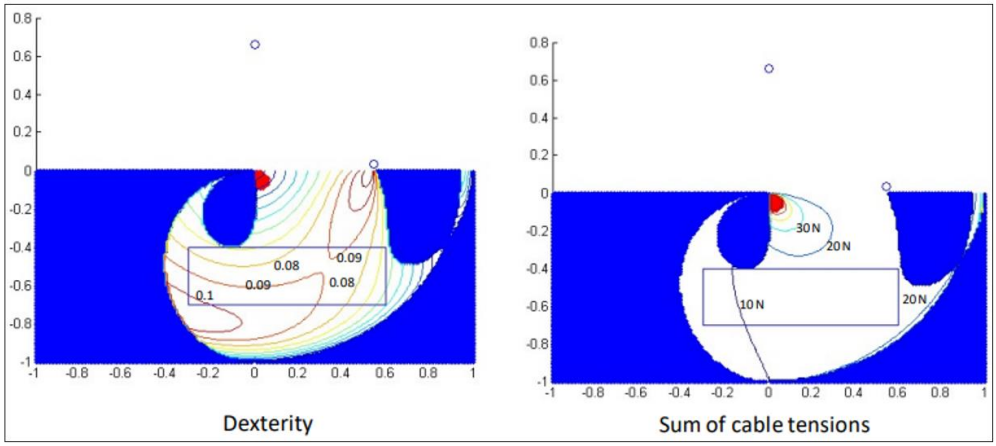

Fig. 15: Results of the optimization process minimizing cable tensions (solution 2)

Table 1: Solutions from the Pareto front

	Dexterity	Cable tensions	x1	y1	x2	y2
1	-0.128	8.3	-0.742	0.005	0.750	0.082
2	-0.084	6.5	0.001	0.660	0.546	0.032
3	-0.127	7.2	-0.840	0.009	0.552	0.036

Table 2: Solutions from the Pareto front of the three degrees of freedom hybrid robot

	Dexterity	Cable tensions	x1	y1	x2	y2	x3	y3
1	-0.053	6.12	-0.601	0.770	0.623	0.266	0.267	0.991
2	-0.044	5.87	-0.045	0.834	0.567	0.256	0.553	0.666

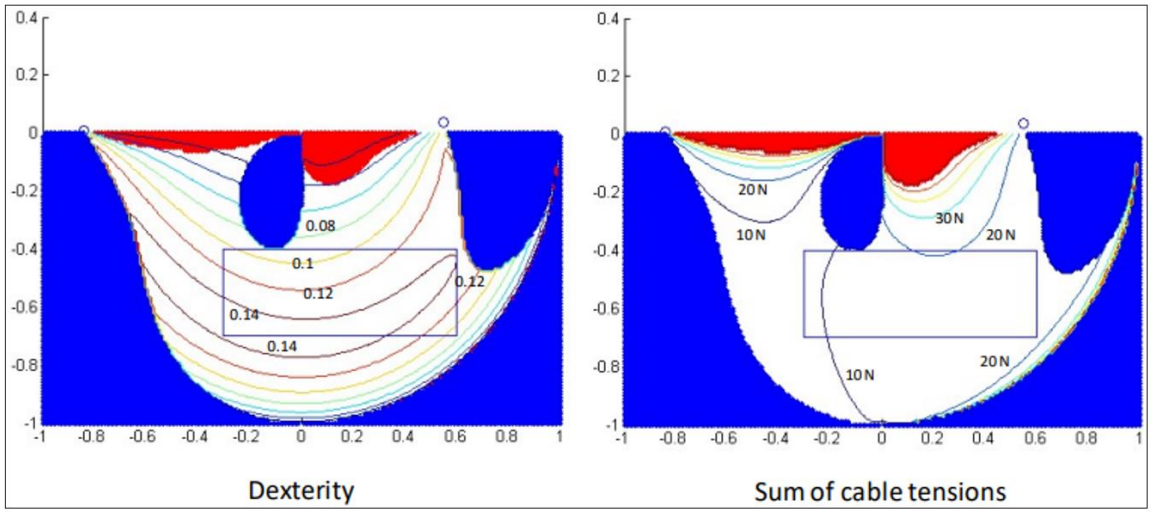

Fig. 16: Results in solution 3

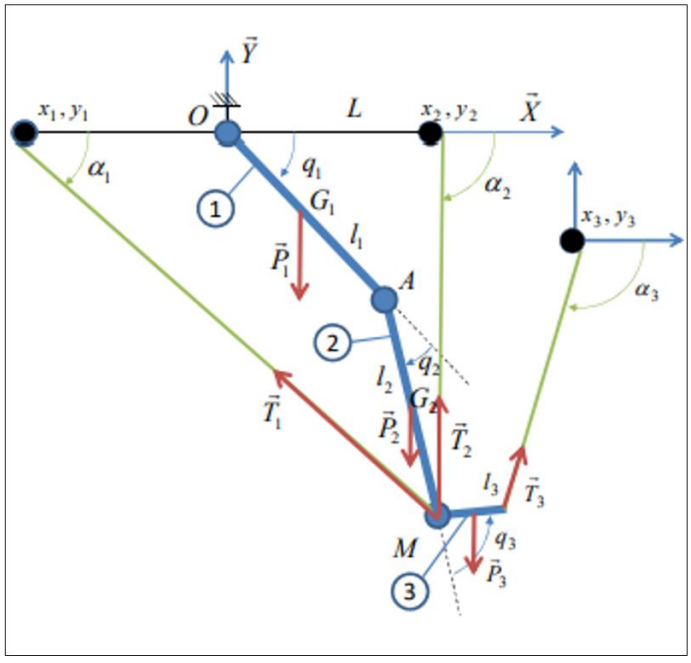

Fig. 17: Three degrees of freedom hybrid robot

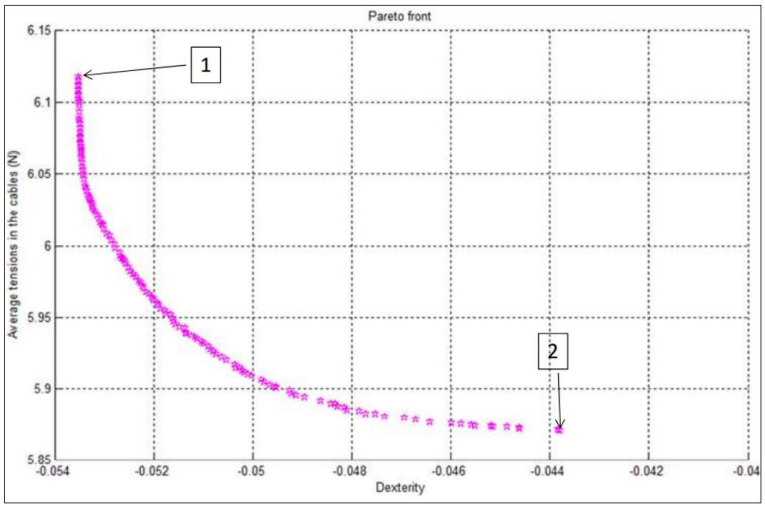

Fig. 18: Pareto front of the three degrees of freedom hybrid robot

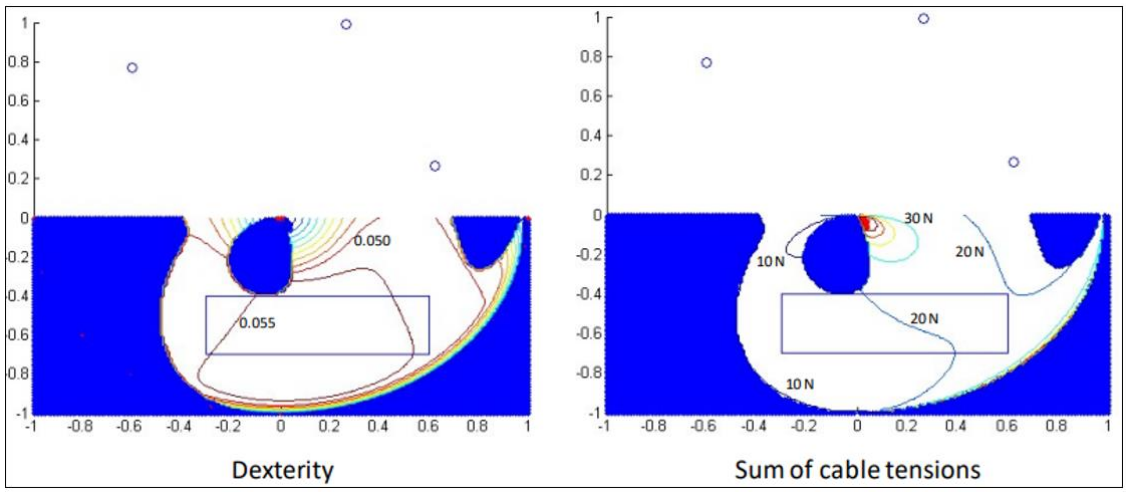

Fig. 19: Results of the optimization process maximizing the inverse of the condition number of the 3 dof hybrid robot (solution 1)

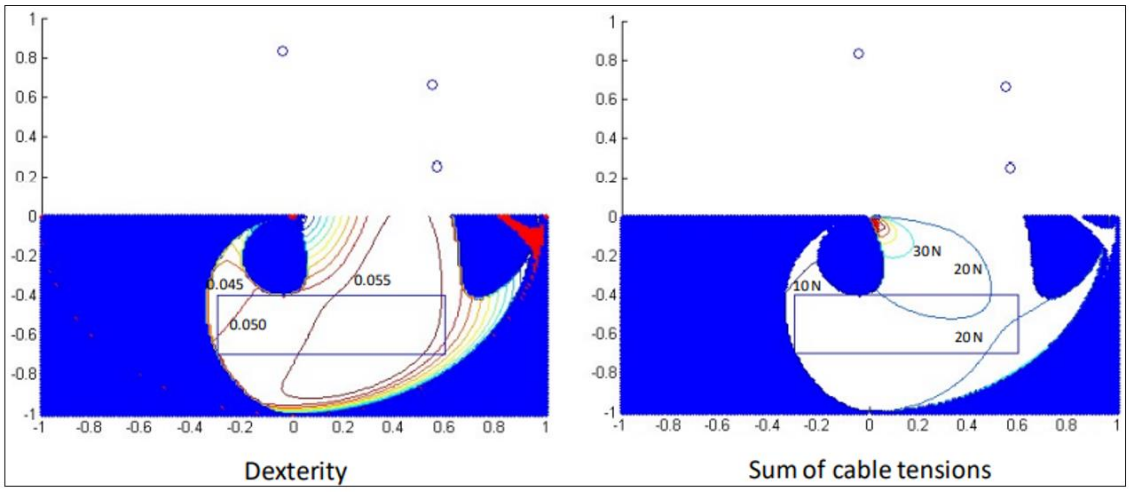

Fig. 20: Results of the optimization process minimizing cable tensions of the 3 dof hybrid robot (solution 2)

Whereas Fig. 20 shows solution 2 where the average cable tension in the workspace is minimized.

Discussion

Singularities in the case of a hybrid cable serial robot are studied. Three types of singularities have been identified and discussed. These singularities are serial singularities present in the boundary of the workspace, parallel singularities in the upper limit of the workspace, and combined singularities corresponding to both cases. In addition, cable tensions are verified, and negative tensions in one or both of the cables have to be avoided. It has been shown that these configurations depend on the geometrical parameters of the serial part of the robot and on the position of pulleys (used to attach cables). They also depend on the mass ratio $\lambda = \frac{m_1}{m_2}$, the higher this ratio the smaller the cable singularity region. Moreover, a region within the workspace where cable tensions increase drastically was identified. This region should be avoided to prevent excessive tensions in the cables. The use of the studied robot in gait rehabilitation was proposed. Results of the optimization of the pulley positions, given a prescribed region for the patient tip, are shown. Two types of results are given, the first one is based on the condition number of the Jacobian matrix and the second one is based on cable tensions. It is shown that minimizing the condition number gives better results than minimizing the cable tensions in terms of making the prescribed region far from singularities. This experiment is also conducted on the three degrees of freedom hybrid robot and has led to the same conclusion.

Conclusion

In this study, the influence of the geometrical parameters as well as the mass ratio on the workspace of the hybrid cable serial robot have been studied. Understanding this influence is useful in the design of such robots that are very promising in the stroke rehabilitation field.

Acknowledgment

This study was supported both by the Ecole Nationale d'Ingenieurs de Monastir and the College of Engineering at the American University of Sharjah. The authors are grateful to their respective institutions for this support.

Author's Contributions

Samir Lahouar: Responsible for the writing, formulation of the problem and the simulation.

Lotfi Romdhane: Responsible for the writing, and the discussion of the results.

Ethics

The authors have no competing interests to declare that are relevant to the content of this study.

References

Angeles, J., & López-Cajún, C. S. (1992). Kinematic isotropy and the conditioning index of serial robotic manipulators. *The international journal of Robotics Research*, *11*(6), 560-571. https://doi.org/10.1177/027836499201100605

Barnett, E., & Gosselin, C. (2015). Time-optimal trajectory planning of cable-driven parallel mechanisms for fully specified paths with G1-discontinuities. *Journal of Dynamic Systems, Measurement, and Control*, *137*(7). https://doi.org/10.1115/1.4029769

Bonev, I. A., Zlatanov, D., & Gosselin, C. M. M. (2003). Singularity analysis of 3-DOF planar parallel mechanisms via screw theory. *J. Mech. Des.*, *125*(3), 573-581. https://doi.org/10.1115/1.1582878

Boudreau, R., & Nokleby, S. (2012). Force optimization of kinematically-redundant planar parallel manipulators following the desired trajectory. *Mechanism and Machine Theory*, *56*, 138-155. https://doi.org/10.1016/J.MECHMACHTHEORY.2012.06.001

Deb, K. (2011). Multi-objective optimization using evolutionary algorithms: an introduction. In *Multi-objective evolutionary optimization for product design and manufacturing* (pp. 3-34). Springer, London. https://doi.org/10.1007/978-0-85729-652-8_1

Firmani, F., & Podhorodeski, R. P. (2009). Singularity analysis of planar parallel manipulators based on forwarding kinematic solutions. *Mechanism and Machine Theory*, *44*(7), 1386-1399. https://doi.org/10.1016/J.MECHMACHTHEORY.2008.11.005

Gosselin, C., & Angeles, J. (1990). Singularity analysis of closed-loop kinematic chains. *IEEE transactions on robotics and automation*, *6*(3), 281-290.

Ismail, M., Lahouar, S., & Romdhane, L. (2016). The collision-free and dynamically feasible trajectory of a hybrid cable–a serial robot with two passive links. Robotics and Autonomous Systems, 80, 24-33. https://doi.org/10.1016/J.ROBOT.2016.03.001Get

Lahouar, S., Ottaviano, E., Zeghoul, S., Romdhane, L., & Ceccarelli, M. (2009). Collision-free path-planning for cable-driven parallel robots. *Robotics and Autonomous Systems*, *57*(11), 1083-1093.Get rights and content. https://doi.org/10.1016/J.ROBOT.2009.07.006

Lahouar, S., Zeghloul, S., & Romdhane, L. (2008). Singularity-free path planning for parallel robots. In *Advances in Robot Kinematics: Analysis and Design* (pp. 235-242). Springer, Dordrecht. https://doi.org/10.1007/978-1-4020-8600-7_25

Li, T., Tang, X., & Tang, L. (2016). Algebraic expression and characteristics of static wrench-closure workspace boundary for planar cable-driven parallel robots. *Advances in Mechanical Engineering*, *8*(3), 1687814016638217. https://doi.org/10.1177/1687814016638217

Litvin, F. L., & Parenti Castelli, V. (1985). Configurations of robot manipulators and their identification, and the execution of prescribed trajectories. Part 1: *Basic concepts*. https://doi.org/10.1115/1.3258706

Liu, X. J., Wu, C., & Wang, J. (2012). A new approach for singularity analysis and closeness measurement to singularities of parallel manipulators. *Journal of Mechanisms and Robotics*, *4*(4). https://doi.org/10.1115/1.4007004

Paul, R. P., & Stevenson, C. N. (1983). Kinematics of robot wrists. *The International journal of robotics research*, *2*(1), 31-38. https://doi.org/10.1177/027836498300200103

Pigani, L., & Gallina, P. (2014). Cable-direct-driven-robot (CDDR) with a 3-link passive serial support. *Robotics and Computer-Integrated Manufacturing*, *30*(3), 265-276. https://doi.org/10.1016/J.RCIM.2013.10.006

Trevisani, A. (2013). Experimental validation of a trajectory planning approach avoiding cable slackness and excessive tension in under constrained translational planar cable-driven robots. In *Cable-Driven Parallel Robots* (pp. 23-39). Springer, Berlin, Heidelberg. https://doi.org/10.1007/978-3-642-31988-4_2

Trevisani, A., Gallina, P., & Williams, R. L. (2006). Cable-Direct-Driven Robot (CDDR) with passive SCARA support: Theory and simulation. *Journal of Intelligent and Robotic Systems*, *46*(1), 73-94. https://doi.org/10.1007/s10846-006-9043-7

Yang, G., Chen, W., & Chen, I. M. (2002, October). A geometrical method for the singularity analysis of 3-RRR planar parallel robots with different actuation schemes. In *IEEE/RSJ international conference on intelligent robots and systems* (Vol. 3, pp. 2055-2060). IEEE. https://doi.org/10.1109/IRDS.2002.1041568

Yoshikawa, T. (1985). Manipulability of robotic mechanisms. *The international journal of Robotics Research*, *4*(2), 3-9. https://doi.org/10.1177/027836498500400201

Zargarbashi, S. H. H., Khan, W., & Angeles, J. (2012). The Jacobian condition number as a dexterity index in 6R machining robots. *Robotics and Computer-Integrated Manufacturing*, *28*(6), 694-699. https://doi.org/10.1016/J.RCIM.2012.04.004

Zhang, N., & Shang, W. (2016). Dynamic trajectory planning of a 3-DOF under-constrained cable-driven parallel robot. *Mechanism and Machine Theory*, *98*, 21-35.

Zou, Y., Zhang, Y., & Zhang, Y. (2012, August). On the Design of Singularity-Free Cable-Driven Parallel Mechanism Based on Grassmann Geometry. In *International Design Engineering Technical Conferences and Computers and Information in Engineering Conference* (Vol. 45035, pp. 851-858). American Society of Mechanical Engineers. https://doi.org/10.1115/DETC2012-71076